THE ASTROPHYSICAL JOURNAL, 203:159–168, 1976 January 1

OPTICAL AND MILLIMETER-WAVE OBSERVATIONS OF THE M8 REGION

CHARLES J. LADA
Center for Astrophysics, Harvard College Observatory and Smithsonian Astrophysical Observatory
T. R. GULL
Kitt Peak National Observatory*
AND
C. A. GOTTLIEB AND E. W. GOTTLIEB
Center for Astrophysics, Harvard College Observatory and Smithsonian Astrophysical Observatory
Received 1975 April 14; revised 1975 June 16

ABSTRACT

Millimeter-wave observations made toward the NGC 6530–M8 star-forming complex are compared with high-quality optical interference-filter photographs of that region taken with the new Kitt Peak 4-m Mayall telescope and the Kitt Peak No. 1 92-cm telescope. Extensive CO observations reveal a large molecular cloud in this direction, within which three bright spots of CO emission are found. Two bright spots are associated in angle with prominent optical features. One of these is coincident with the star Herschel 36 and the well-known Hourglass Nebula, and the second appears coincident in angle with a bright-rimmed structure shown to be an ionization front southeast of Herschel 36. Emission from H_2CO at 140.8 GHz and H_2O at 22.2 GHz has been detected from this last bright spot but not from the other two. The third bright spot does not seem to be associated with any visible nebular feature. Carbon monoxide, radio continuum, and optical Hα emission are found to be very similar in angular distribution throughout M8.

The kinematics of the molecular cloud are studied, and we find that the radial velocity of CO emission varies smoothly across the cloud, but it is difficult to interpret this in terms of coherent mass motion of the entire cloud. Analysis of available radial-velocity data for the H II region shows that the ionized gas is approaching the Earth at a velocity of 7 km s^{-1} with respect to the molecular cloud.

Analyses of CO, radio continuum, and, especially, optical data indicate that Herschel 36 is the most likely ionizing source for most of the M8 H II region. Comparison of optical and radio observations suggests a geometrical model for the region, which places the H II region at the front edge of the molecular cloud. Further considerations indicate that the M8 molecular cloud, the M8 H II region, the young cluster NGC 6530, and the Sgr OB1 association appear to be related in a geometrical evolutionary sequence with cloud evolution, and possibly star formation, proceeding inward with time from the position of the foreground star cluster to the position of the molecular cloud.

Subject headings: interstellar molecules: — nebulae: individual

I. INTRODUCTION

The Lagoon Nebula (M8) is a bright emission nebula located behind the extremely young (2×10^6 yr) open cluster NGC 6530. This cluster, which is at the center of the Sgr OB1 association, has been studied extensively (e.g., Walker 1957; van Altena and Jones 1972). The H II region M8 has also been studied optically by a number of investigators (Foukal 1969; Bohuski 1973*a*, *b*; Dopita 1974) and has been found to be very similar in excitation requirements to the Orion Nebula. However, radio observations of this source are few and consist mostly of continuum maps made at centimeter wavelengths (e.g., Shaver and Goss 1970) and detections of recombination lines toward the continuum peak (e.g., Reifenstein *et al.* 1970; Wilson *et al.* 1970). To date, no map of radio line emission has been reported.

Close to the peak of radio continuum emission and the center of optical emission lie two very interesting objects: the Hourglass Nebula and the O7 star Herschel 36. Woolf (1961) has suggested that Herschel 36 is a newly born star recently emerged from its cocoon and is responsible for ionizing the Hourglass Nebula. Infrared observations indicate the presence of dust near Herschel 36 (Woolf *et al.* 1973; Loewenstein *et al.* 1974). The detection of H_2CO at 6-cm wavelength (Zuckerman *et al.* 1970) and of millimeter-wave HCN emission (Giguere *et al.* 1973) reveals the presence of a molecular cloud in the direction of this star, and examination of the extinction around the entire M8 region shows a large dark cloud located behind NGC 6530 (The 1960). The proximity of Herschel 36, NGC 6530, the Lagoon Nebula, and the extended dark cloud suggests that the M8 complex is

* Operated by the Association of Universities for Research in Astronomy, Inc., under contract with the National Science Foundation.

a region where star formation has recently taken place and that it may still be active. Observations of similar dark molecular clouds, particularly M17 (Lada *et al.* 1974*a*; Lada and Chaisson 1975), show that detailed mapping of molecular lines can be extremely useful for detecting and studying regions of incipient star formation, especially since some of the more interesting regions are often not coincident in angle with optical emission.

In this paper, we report the initial results of an extensive radio and optical study of the M8 complex. Emission lines of the $J = 1 \rightarrow 0$ rotational transition of ^{12}CO and ^{13}CO have been mapped throughout the central regions of the M8 Nebula. We compare these maps with high-quality interference-filter photographs of the region made with the new 4-m Mayall reflector and the No. 1 92-cm telescope at Kitt Peak National Observatory in order to study both the nature of the star-forming complex and the relationship of the molecular cloud to the H II region. With these observations as a basis, a phenomenological model for the evolutionary history of the entire NGC 6530–M8 region is constructed.

II. EQUIPMENT

The millimeter-wavelength observations were made on 1974 June 24–July 2, 1974 October 31–November 12, and 1975 February 4–13 with the 16-foot (5-m) millimeter-wave telescope at the McDonald Observatory near Fort Davis, Texas.[1] The equipment and observing procedure have been described elsewhere (Lada *et al.* 1974*a*). The single-sideband system temperature measured by the hot-cold load technique was 2000 K for ^{12}CO, 2200 K for ^{13}CO, and 2400 K for H_2CO at 140.8 GHz. Multiplying factors derived by Davis and Vanden Bout (1973) were used to convert the measured ^{12}CO antenna temperatures to Rayleigh-Jeans brightness temperatures.

The H_2O observations were made on 1975 March 29 with the 120-foot (37-m) telescope at the Haystack Observatory[2] in Westford, Massachusetts. The equipment has been described elsewhere (Lada *et al.* 1974*b*). The system temperature was 125 K, and the autocorrelator bandwidth was 6.67 MHz (89.9 km s^{-1}). The observations were made in the total-power mode, the final spectrum being an average of many separate pairs of 2-min on-source and 2-min off-source integrations.

Direct photographic plates of the M8 region were taken at Kitt Peak with the No. 1 92-cm telescope during the summer of 1973 and the 4-m telescope during the summer of 1974. Three-period interference filters with excellent rejection outside the central bandpass were utilized to isolate specific optical emission lines and several portions of the continuous spectrum.

The prime-focus camera (focal ratio F/2.6) of the 4-m telescope was used in combination with 90 Å wide interference filters (full width at half-intensity) measuring 100 mm × 100 mm in size. One filter isolated Hα (λ6563) with the [N II] lines (λ6548 and λ6584), and another isolated the continuum centered about λ6424.

Narrower bandpass interference filters ($\Delta\lambda$ = 6–20 Å) were employed in combination with the No. 1 92-cm telescope to isolate single emission lines. The slower focal ratio (F/7.5) of this telescope allowed use of filters that passed the Hα emission while rejecting the nearby [N II] emission. However, since the exposure time for recovering nebulae increases as the square of the focal ratio, a two-stage image intensifier was utilized to increase both the detective quantum efficiency and the blackening rate of the exposure. Resultant plates, though limited in image diameter by the modulation transfer function of the image intensifier, were exposed in roughly one-tenth the time necessary at the 4-m prime focus. Exposure times of all plates recorded ranged from a few minutes to 1 hour. Parameters of the specific filter photographs reproduced in the figures of this article are described in the figure legends. Typical transmissions for all filters were 50 percent.

III. OBSERVATIONS

a) Morphology of the Molecular Cloud

We have mapped the emission lines of ^{12}CO and ^{13}CO in 90 and 15 respective locations distributed throughout the central regions of the Lagoon Nebula. Figure 1 (Plate 5) is a contour map of peak ^{12}CO brightness temperature in the velocity range between 10 and 17 km s^{-1}, superposed on a prime-focus optical continuum photograph made with the Mayall 4-m telescope through a 90 Å wide interference filter centered at λ6424. The CO observations used to construct this map were made at 1′.5 spacings. Additional observations outside the 5 K contour level in Figure 1 indicate that generally weaker CO emission is extended over a larger area, probably similar in size to the dark nebula located behind M8 (The 1960). The CO emission at a 10 K brightness-temperature level covers an area roughly 20′ × 12′, or 12 × 7 pc at the distance of M8.

Three bright spots of CO emission have been discovered in the central regions of M8; their positions are listed in Table 1.

Bright Spot 1 is centered on the well-known Hourglass Nebula and the O7 star Herschel 36. Both near- (10–20 μ) and far- (~90 μ) infrared radiation have been observed near Herschel 36 (Woolf *et al.* 1973; Loewenstein *et al.* 1974). Additionally, a weak emission line of $H^{12}CN$ and a weak 6-cm-wavelength

[1] The Millimeter Wave Observatory is operated by the Electrical Engineering Research Laboratory, University of Texas at Austin, with support from the National Aeronautics and Space Administration, the National Science Foundation, and McDonald Observatory. The instrumentation used for spectral-line observations with this antenna was developed jointly by the University of Texas, Bell Telephone Laboratories, and the Radio Astronomy Division of the Center for Astrophysics.

[2] The Haystack Observatory is operated by the Northeast Radio Observatory Corporation with support from the National Science Foundation.

TABLE 1

COORDINATES OF CO BRIGHT SPOTS

Bright Spot	Pointing Position (1950) α	δ
1.....	$18^h00^m35^s$	−24°23′20″
2.....	18 01 02	−24 27 50
3.....	18 01 17	−24 23 20

H_2CO absorption line have both been seen in this direction. We searched for, but did not detect, emission from H_2CO at 140.8 GHz, with the result that T_B (H_2CO) $\lesssim$ 0.5 K toward Herschel 36.

Bright Spot 2, southeast of Herschel 36, is near a conspicuous bright-rimmed structure in the nebula. Loewenstein *et al.* (1974) found a 90-μ infrared source close to this bright spot. Observations at other infrared wavelengths have yet to be made. We have detected emission from the 140.8-GHz transition of H_2CO, indicating a molecular hydrogen density of $\gtrsim 10^4$ cm^{-3} in this region. The line parameters for the H_2CO feature are $T_B = 1.3 \pm 0.1$ K, $V_{LSR} = 12.77 \pm 0.07$ km s^{-1}, and $\Delta V = 1.4 \pm 0.2$ km s^{-1}. The H_2CO velocity agrees well with the ^{13}CO velocity of 12 ± 1 km s^{-1}. The H_2CO line is a factor of 2 narrower than ^{13}CO and 2.5 times narrower than ^{12}CO. We have also detected a single H_2O feature at 10.9 km s^{-1} toward the position given in Table 1 for Bright Spot 2. Since we did not map this feature, we cannot rule out the possibility that a strong H_2O source was on the edge of the antenna beam. Spectra of ^{12}CO, ^{13}CO, H_2CO, and H_2O taken toward Bright Spot 2 are shown in Figure 2.

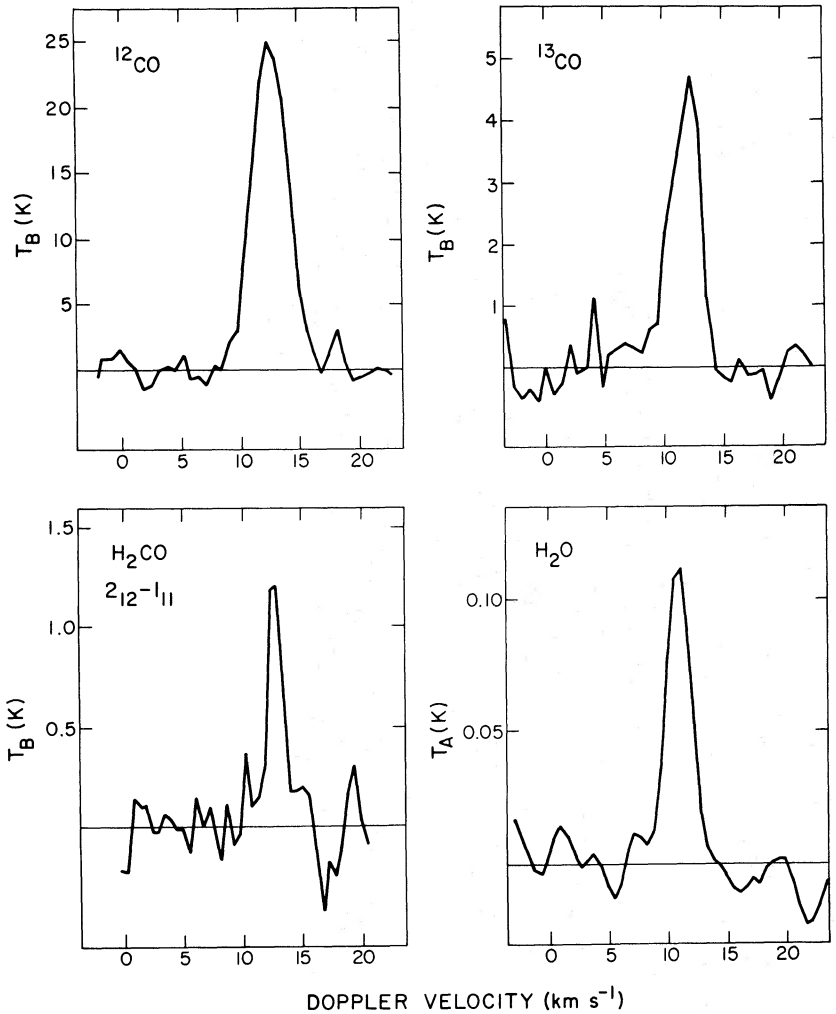

FIG. 2.—Spectra of ^{12}CO, ^{13}CO, H_2CO (2_{12}–1_{11}), and H_2O made when the antenna was pointed toward Bright Spot 2. The temperature scales for the ^{12}CO, ^{13}CO, and H_2CO spectra are apparent Rayleigh-Jeans brightness temperatures referred to outside the Earth's atmosphere. The temperature scale for the H_2O spectrum is the antenna temperature uncorrected for atmospheric absorption. The velocity scales are referred to the LSR and to a line rest frequency of 115,271.201 MHz for ^{12}CO; 110,201.40 MHz for ^{13}CO; 140,839.529 MHz for H_2CO; and 22,235.078 MHz for H_2O. The instrumental resolution is 0.65 km s^{-1} for ^{12}CO, 0.68 km s^{-1} for ^{13}CO, 0.53 km s^{-1} for H_2CO, and 2.25 km s^{-1} for H_2O. Linear baselines have been removed.

Bright Spot 3, approximately 9′ east of Herschel 36, is close in angle to a dense portion of the young cluster NGC 6530. Searches for near-infrared radiation and molecular emission from molecules other than CO and H_2CO have not yet been made. We looked for, but could not detect, H_2CO at 140.8 GHz toward Bright Spot 3, implying that $N_{H_2} \lesssim 10^4$ cm^{-3}. Ninety-micron emission may have been detected near this bright spot but does not appear spatially coincident with the CO peak (Loewenstein *et al.* 1974).

The spatial appearance of the CO emission within the 10 K contour is very similar to those of Hα (§ IV) and radio continuum emission (Ball 1969; Shaver and Goss 1970). Within the 15 K contour, the CO emission region is similar in shape to the 90-μ emission (Loewenstein *et al.* 1974).

In all the bright spots, ^{13}CO has been detected close to the peak positions. The ratio of ^{12}CO to ^{13}CO integrated brightness temperatures at Bright Spot 1 is 9 ± 2; at Bright Spot 2 and Bright Spot 3, these ratios are 7 ± 2 and 4.1 ± 0.3, respectively. All these ratios are slightly greater than those observed toward similar bright spots in M17 (Lada *et al.* 1974*a*), Orion A (Liszt *et al.* 1974), NGC 1333 (Lada *et al.* 1974*b*), and other sources, indicating lower column densities of CO toward M8. Assuming that a density of 10^3 cm^{-3} for molecular hydrogen is necessary to excite the CO to observable levels, the total mass of the molecular cloud within the 10 K contour in Figure 1 is $\sim$2000 $M_\odot$ (for a cloud depth of 1 pc).

We have also found narrow ^{12}CO emission lines toward M8 from a cloud whose velocity is close to 28 km s^{-1}. This cloud is approximately 9′ × 4′ in extent and is centered near $\alpha_{1950} = 18^h01^m29^s$, $\delta_{1950} = -24°26'41''$. The cloud does not appear coincident with any visible nebular features; however, our map of it is incomplete, and more observations are required before its nature can be examined. The line parameters for ^{12}CO at the center position of this cloud are $T_B = 11.1 \pm 0.6$ K, $V_{LSR} = 27.93 \pm 0.04$ km s^{-1}, and $\Delta V = 1.49 \pm 0.09$ km s^{-1}.

b) Kinematics in the Molecular Cloud

In M8, as in most other molecular clouds, the velocity structure of CO emission is complex. In order to study the kinematics of the M8 molecular cloud, we have constructed a number of velocity-angle maps taken through selected positions in the cloud. The velocity-versus-angle contour plots were made with a computer program written by John Ball, which uses a (sin x)/x function for interpolating both the velocity and the angle coordinates.

Figure 3 shows an east–west strip through the M8 molecular cloud made at a declination close to that of Herschel 36. This diagram is a plot of all the ^{12}CO line profiles observed at $\delta_{1950} = -24°23'20''$ and shows the presence of two distinct features, at $\sim$11 km s^{-1} and $\sim$16 km s^{-1}. These features are clearly separated in angle as well as in velocity. Emission at $\sim$11 km s^{-1} is coincident with Bright Spot 1 and has decreased to half its peak intensity 4′ east. Emission at $\sim$16 km s^{-1}

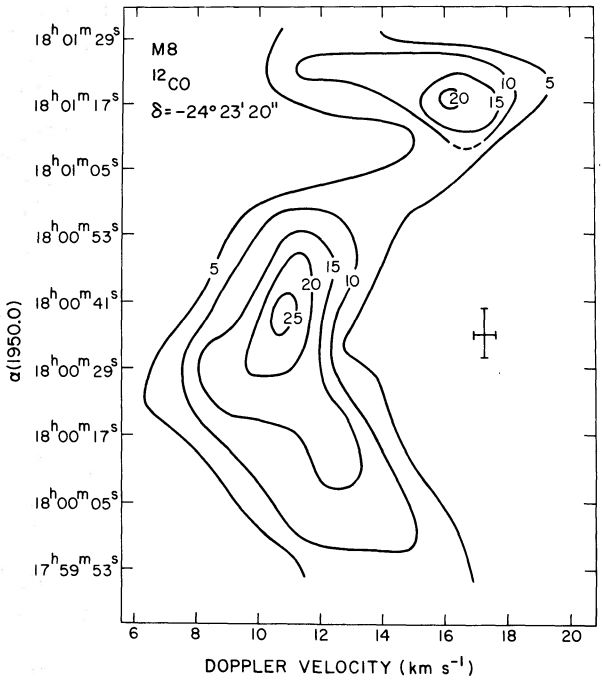

FIG. 3.—Velocity-angle contour map of equal ^{12}CO Rayleigh-Jeans brightness temperature along an east–west line at $\delta_{1950} = -24°23'20''$ passing through Bright Spot 1 and Bright Spot 3 in M8. The temperature units are the same as in Fig. 1.

picks up near $\alpha_{1950} = 18^h01^m12^s$ and peaks on Bright Spot 3. This behavior can be compared with Figure 1. The apparent separation in both velocity and angle of CO emission from Bright Spot 1 and Bright Spot 3 would seem to imply that the CO emission was originating in two separate clouds along the line of sight toward M8. Examination of Figures 4, 5, and 6 indicates that this is not necessarily the case. Figure 4 shows ^{12}CO line profiles observed along a north–south strip at the approximate right ascension of Bright Spot 3. There seems to be a smooth gradient of radial velocity, with velocities ranging from 17.5 km s^{-1} about 1′.5 north of Bright Spot 3 to $\sim$14 km s^{-1} 2′ south of it. Farther south, the velocity remains constant near 14 km s^{-1} until, at $\delta_{1950} \approx -24°29'$, an additional component near 18 km s^{-1} appears.

As can be seen in Figure 1, Bright Spot 1 and Bright Spot 3 are apparently connected by a bridge of CO emission that contains Bright Spot 2 near its center. Figure 5 is an east–west strip containing ^{12}CO profiles observed at the approximate declination of Bright Spot 2 and the emission bridge. Figures 4 and 5 overlap at $\alpha_{1950} = 18^h01^m17^s$ and $\delta_{1950} = -24°27'50''$. The radial velocity in the cloud varies smoothly from that point through Bright Spot 2 to the right ascension of Bright Spot 1, ranging from $\sim$14 to 11 km s^{-1}. Almost no change in radial velocity is apparent in Figure 6, which is a north–south strip through Herschel 36. Together, Figures 3 through 6 show a smooth gradient in radial velocity from Bright Spot 3 around

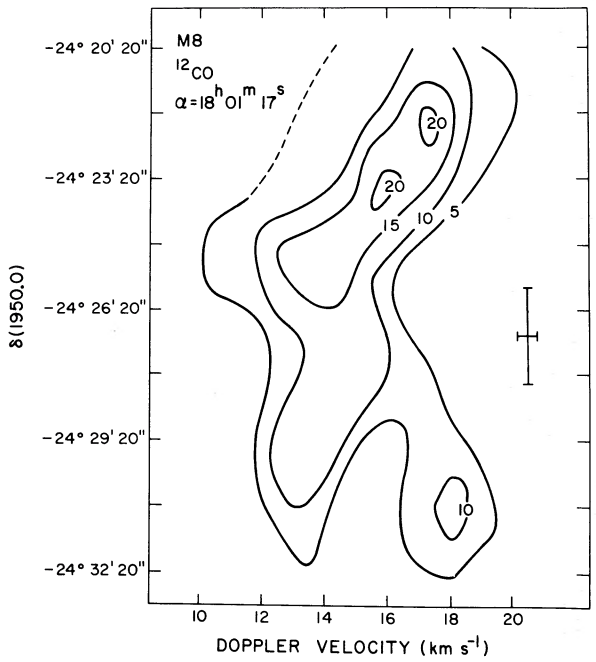

FIG. 4.—Velocity-angle contour map of ^{12}CO emission made along a north–south line at $\alpha_{1950} = 18^h01^m17^s$ and passing through Bright Spot 3. The temperature units are the same as in Fig. 1.

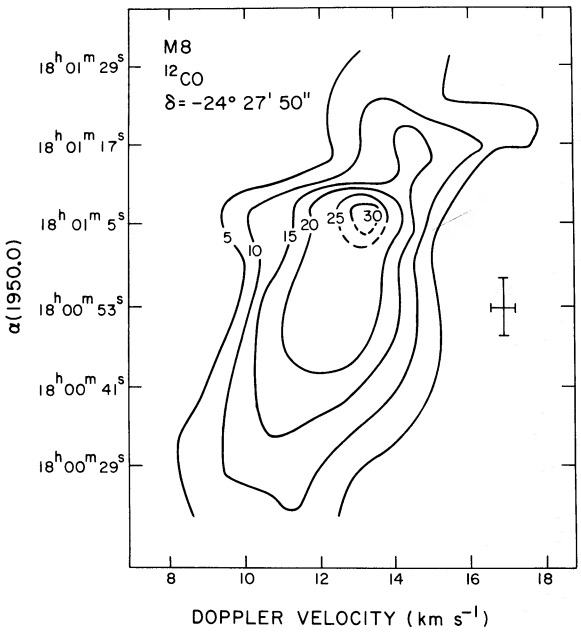

FIG. 5.—Velocity-angle contour map of ^{12}CO emission made along an east–west line at $\delta_{1950} = -24°27'50''$ and passing through Bright Spot 2. The temperature units are the same as those of Fig. 1.

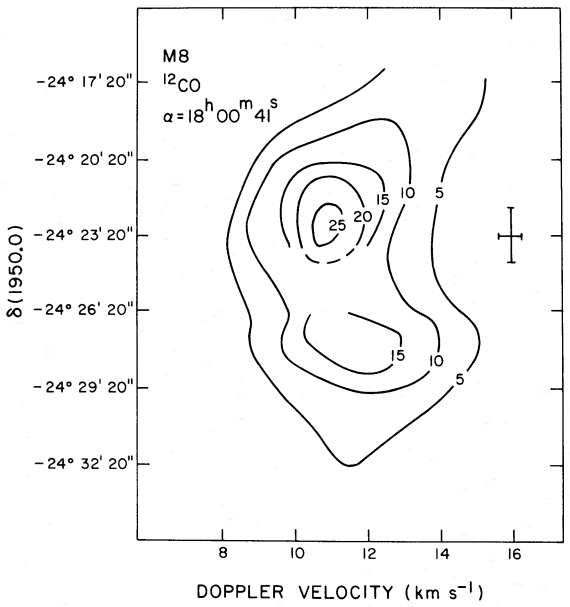

FIG. 6.—Velocity-angle contour map of ^{12}CO emission made along a north–south line at $\alpha_{1950} = 18^h00^m41^s$ and passing through Bright Spot 1. The temperature units are the same as those of Fig. 1.

the emission bridge to Bright Spot 1, varying from 17 to 10 km s^{-1}. This is perhaps suggestive of a physical connection between the three spots. However, interpretation of the observed radial-velocity behavior in terms of coherent mass motion of the entire cloud seems difficult. The CO emission near Herschel 36 appears to be blueshifted with respect to the rest of the molecular cloud, as indicated in Figure 3 and possibly in Figure 6. Figure 4 might best be explained by a rotation of part of the cloud about Bright Spot 3 around an east–west axis.

c) *Morphology of the Ionized Regions*

In order to investigate the ionization structure near the M8 molecular cloud, we have taken a number of narrow-band interference-filter photographs of the central regions of M8 using an image intensifier at the No. 1 92-cm telescope at Kitt Peak. Here we report some preliminary findings of our study.

Figure 7 is a schematic drawing showing the locations of the most important optically visible features pertinent to the discussion in this paper. The stars 9 Sgr, 7 Sgr, Herschel 36, MWC 280, W54, and LkHα 112 and the Hourglass Nebula are indicated. In addition, two interesting bright-rimmed features are identified—the Southeast Bright Rim (SEBR) and the Super Hourglass Structure (SHGS), a large-scale rim-like structure similar in shape to but different in orientation from the Hourglass Nebula. Figure 7 should be used as a key to studying our optical photographs and the discussion that follows.

Figure 8 (Plate 6) shows four interference-filter photographs centered near the wavelengths of atomic emission lines of increasing ionization potential,

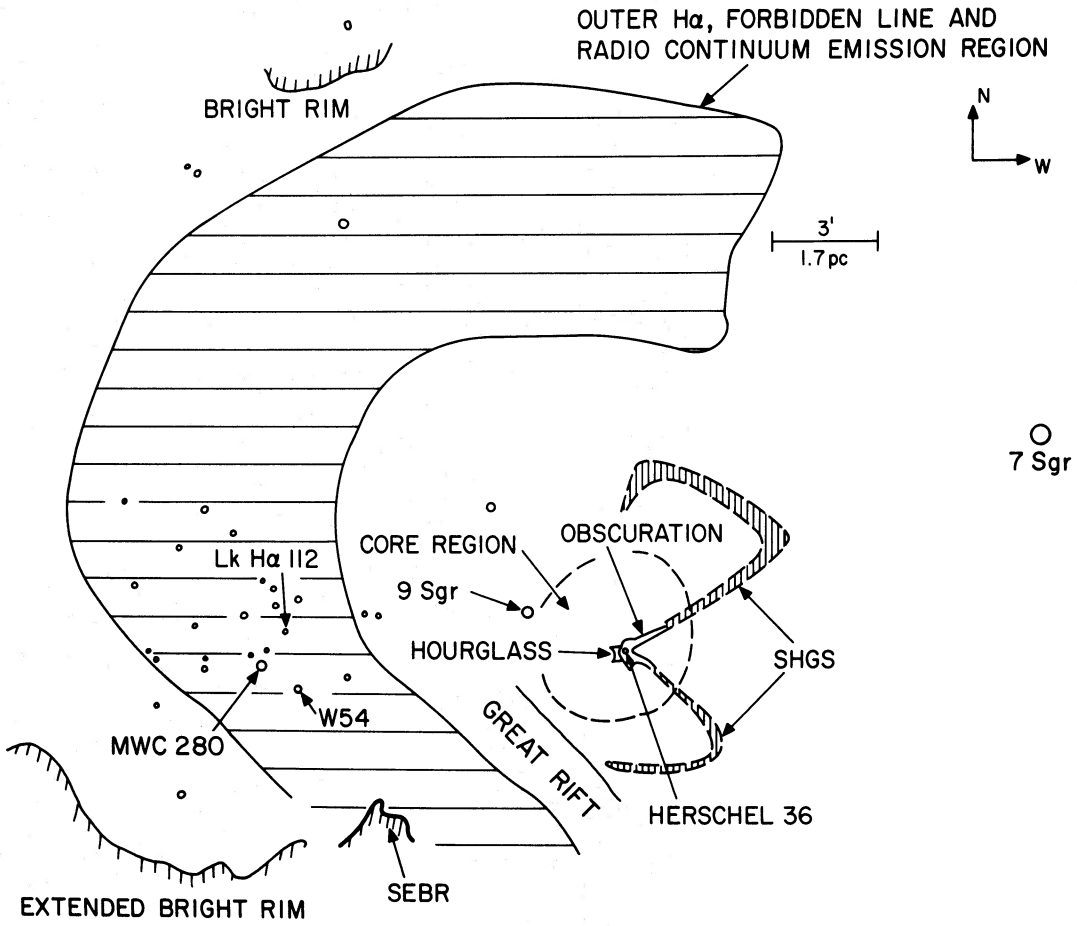

FIG. 7.—Schematic drawing (to scale) of the prominent optical features of M8 pertinent to the discussion in this paper

[O I], [S II], [N II], and [O III]. Figure 8*a* is a 60-min exposure of [O I] emission at λ6300 taken through a 6 Å wide filter. The Hourglass Nebula, SEBR, and SHGS are weakly visible (see Fig. 7). However, the last two features are more apparent in the photographs of [S II] and [N II] emission, Figures 8*b* and *c*. Although not reproduced here, photographs of [O II] emission at λ3727 are similar to the [N II] and [S II] pictures. Comparison of Figures 8*a* through 8*c* with the continuum photograph of Figure 1 and continuum photographs at λ6424 shows that although these two rim features are bright in forbidden radiation of [O I], [S II], and [N II], they are not seen in continuum emission, indicating that SEBR and SHGS are ionization features; that is, the radiation we observe originates in ionized gas and is not dust-scattered continuum emission. Moreover, the angular structure of [S II] and [N II] emission is different from that of the continuum emission. This suggests that the emission-line radiation is also not scattered radiation but originates locally.

Bohuski (1973*b*) has estimated the electron-density distribution through selected portions of the SHGS, using observations of the density-sensitive doublet [S II] λλ6717, 6731. These observations showed an enhancement of electron density at the SHGS. Through a portion of the southwest rim of SHGS, the electron density was found to increase from a general nebular background of ~ 500 to ~ 5500 cm^{-3} at the most dense section of the rim. Two scans through the northwest rim of the SHGS revealed an enhanced density of ~ 3500 cm^{-3} at the rim, compared with ~ 1000 cm^{-3} for the surrounding nebular environment, thus confirming the nature of the SHGS as an ionization feature. Similar measurements have not been made toward the SEBR.

Even though the SHGS and the SEBR are ionization features, they appear to be of different morphological character. The SEBR is an ionization front at the interface of a dense dust cloud, the dimensions of which are larger than the bright-rim feature itself, and therefore the ionization front is probably photon-bounded. The SHGS is a filamentary ionization feature, one in which the dimensions of the region of forbidden-line emission are roughly comparable to those of the material available for ionization, so the SHGS is probably matter-bounded. Good examples of such filamentary structures in other H II regions can be

found in similar photographs of Orion A (Gull 1974, 1975) and, especially, M17 (see, for example, Gull and Balick 1974), where the filaments are observed edge-on and not face-on as in M8. These filamentary features are usually regions of enhanced density, which are manifestations of inhomogeneities in H II regions.

Examination of Figures 1, 8*b*, and 8*c* shows that the material in that part of the SHGS that is closest to Herschel 36 appears in absorption rather than emission (see also Fig. 7). This could be due in part to the surface brightness of [N II] and [S II] emission in the SHGS being lower than that of similar emission originating in the core region of M8. This absorbing matter is partly responsible for the 3.5-mag extinction observed toward Herschel 36 (Woolf 1961).

Figures 1 and 8 reveal that the most highly ionized emission, the brightest forbidden-line emission, and the brightest continuum emission from M8 originate in a core about 5′ in diameter centered near Herschel 36 (see Fig. 7). Bohuski (1973*b*) found that the electron density decreases from $\sim 4200\ \mathrm{cm}^{-3}$ near the Hourglass Nebula to $\sim 1000\ \mathrm{cm}^{-3}$ at the edge of the core region.

Figure 8*d* is a photograph of [O III] emission taken through a 20 Å wide filter centered at λ5007. The [O III] emission is most prominent in the core region of M8. Thus, the emission is similar in extent to the brightest regions of [N II] and [S II] emission and covers a slightly larger area than the optical continuum emission seen in Figure 1. The [O III] emission, as well as the core region, is extended over an area comparable to that of most intense radio continuum emission. We note that neither the SHGS nor the SEBR is visible in [O III] emission. Furthermore, the obscuration associated with the SHGS near Herschel 36 and seen in Figures 1 and 8*a*–8*c* is very weak in the [O III] photograph.

IV. COMPARISON OF RADIO, OPTICAL, AND INFRARED OBSERVATIONS

a) The Hourglass Region and Bright Spot 1

Figure 9 (Plate 7) is a superposition of our ^{12}CO map on a photograph of Hα + [N II] emission taken at the prime focus of the 4-m Mayall telescope through a 90 Å wide narrow-band interference filter centered at λ6563.

As mentioned earlier, Bright Spot 1 peaks very near Herschel 36 and the Hourglass Nebula; however, around this peak is a broad plateau of 20 K CO emission, which is comparable in extent to the SHGS, maximum radio continuum, and 90-μ infrared emission but is slightly more extended than the core of [S II], [N II], and [O III] emission shown in Figures 8*b*–8*d*.

Although we cannot conclusively determine with our data alone whether the CO emission comes from in front, within, or behind the H II region around Herschel 36, comparison of our observations with nebular extinction and recombination-line measurements indicates that the molecular cloud is most probably behind the H II region.

Gebel (1968) has determined a nebular extinction of $A_V = 0.46$ mag for the M8 H II region. With a constant gas-to-dust ratio of $N_{\mathrm{total}} = N(\mathrm{H}) + 2N(\mathrm{H_2}) = 2 \times 10^{21}\ \mathrm{cm}^{-2}\ \mathrm{mag}^{-1}$; a C to H ratio of 4×10^{-4}, and the assumptions that all the carbon is in the form of CO and all the hydrogen is in the form of H_2, Gebel's measurement would predict an upper limit to the CO column density of $N(\mathrm{CO}) \lesssim 3.7 \times 10^{17}\ \mathrm{cm}^{-2}$, compared with $N(\mathrm{CO}) \gtrsim 2 \times 10^{18}\ \mathrm{cm}^{-2}$ derived from our observations, implying that the H II region is in front of the molecular cloud.

The H 109α radio recombination line has been observed toward Herschel 36 and has a radial velocity of $3\ \mathrm{km\ s}^{-1}$ (Reifenstein *et al.* 1970; Wilson *et al.* 1970). In addition, Bohuski (1973*a*) has measured the velocities of Hα emission at 18 locations in the core region of M8. The average velocity of the Hα emission was found to be $0.9 \pm 4.2\ \mathrm{km\ s}^{-1}$ with respect to the local standard of rest (LSR), in reasonable agreement with the recombination-line velocity. This implies that the ionized material from the H II region is approaching us with a velocity of $\sim 7\ \mathrm{km\ s}^{-1}$ with respect to the CO cloud. This observation could be explained by a model in which the molecular cloud was behind the H II region. In the framework of such a model, the exciting star or stars of the H II region would be located near the front edge of the molecular cloud. To maintain pressure equilibrium with the surrounding medium, the hot ionized gases of the H II region will expand in the direction of least resistance. Since the dense molecular cloud offers a barrier to free expansion of the H II region in that direction, the hot gas will stream away from the molecular cloud and, in the case of M8, toward the observer. Similar models have been proposed to explain the velocities observed toward Orion A (Zuckerman 1973; Balick *et al.* 1974) and the morphology of the M17 (Lada 1975) and NGC 2024 (Grasdalen 1974) molecular-cloud–H II region associations.

Although the details are, at present, unknown, the morphological similarity of the enhanced CO emission with the radio continuum, far-infrared, and optical forbidden-line radiation suggests that the exciting source(s) responsible for creating the H II region are also heating the molecular cloud at the cloud–H II region interface. If this interpretation of the enhancement of ^{12}CO emission (which is admittedly based on a guilt-by-association argument) can be shown to be correct, then Bright Spot 1 will be representative of a class of CO bright spots different from what is usually observed. The enhanced temperature is not due to heating by a young, hot, embedded star recently condensed from still collapsing cloud material centered on the bright spot. Instead, Bright Spot 1 is being heated by one or more stars that are currently at the edge of the molecular cloud and have moved away from and/or dissipated much of the embryonic material from which they formed. The presence of the H II region and the SHGS near the core of M8 indicates that disruption and destruction of the molecular cloud are still in progress. However, it is not clear that our guilt-by-association argument relating heating of

Bright Spot 1 with the disruption of the molecular cloud is correct. Orion A and M17 are also being dissipated in a similar manner to M8, yet the bright spots of CO emission in these clouds (OMC-1, OMC-2, M17 SW, M17 N) are associated with discrete embedded sources. In fact, if M17 were observed from a direction in which the H II region was seen in front (and not to the side) of the molecular cloud, the CO bright spot (M17 SW) would appear nearly coincident with the hot H II region.

Our picture of M8 is somewhat dependent on the molecular cloud being located behind the H II region, a fact we cannot conclusively establish with currently available data. Maps of radio recombination lines, optical emission, and 6-cm H_2CO absorption lines of this source would be useful in determining the relative H II region–molecular-cloud geometry, but are not available at this time.

b) The Southeast CO Bright Spot

Figure 9 shows that the southeast CO bright spot is apparently spatially coincident with the Southeast Bright Rim discussed in § III*c*. Although it may be fortuitous, the angular coincidence is suggestive of a physical association. Enhanced ^{12}CO emission, and therefore enhanced kinetic temperature of the cloud, could result from heating of the molecules via some interaction with the ionization front or the ultraviolet photons emitted by the source responsible for the ionization front itself (perhaps the O4f star 9 Sgr). If the CO emission is originating from the dark-cloud structure associated with the SEBR, then we would be observing a molecular hot spot being heated from the outside rather than internally, similar to Bright Spot 1.

We might expect Bright Spot 2 to be an infrared source whether it is being heated externally or internally. However, the character of such emission would be different for each case. If Bright Spot 2 is being heated externally, then the infrared emission would probably be extended and similar in spatial distribution to the visible bright rim. If it is being heated internally, we would expect to find near-infrared point sources within the cloud boundary and far-infrared emission extended and distributed around these sources. A 90-μ emission peak has recently been observed near Bright Spot 2 by Loewenstein *et al.*, but their angular resolution was too coarse to determine the nature and extent of the emission near the optical bright rim. Detection of a point source or sources of near-infrared emission (i.e., 2, 3, 5, 10, or 20 μ) would enable us to determine if internal sources heat Bright Spot 2. Although such observations have not yet been made, the discovery of an H_2O source toward Bright Spot 2 suggests that an infrared point source might be present. The observation that the SEBR may be part of a larger bright-rimmed feature (see Figs. 7 and 9) extending a few parsecs east of the SEBR might indicate that the angular coincidence of Bright Spot 2 with the SEBR is only apparent and not physical. Infrared observations of the type discussed above are necessary before any firm conclusions can be made about the nature of Bright Spot 2.

c) The Eastern CO Bright Spot

Bright Spot 3, the eastern CO bright spot, does not appear to be associated with any obvious nebular feature. However, it is close in angle to a dense portion of the cluster NGC 6530 and is angularly coincident with the star W54 (Walker 1957), which has a 62 percent probability of being a member of NGC 6530 (van Altena and Jones 1972). Also near Bright Spot 3 are the stars LkHα 112 (W58) and MWC 280 (W65), both Hα emission-line stars with spectral types B2 and B0 and cluster-membership probabilities of 80 and 1 percent, respectively. At present, it would be difficult to determine which star, if any, is associated with Bright Spot 3. It would not be surprising to find a CO emission peak near emission-line stars, since CO has been detected toward many Ae and Be stars (Loren *et al.* 1973). It is also possible that a star, currently obscured from view, has recently formed within Bright Spot 3 and has begun to heat its embryonic cloud. Infrared mapping would indicate if this were possible. If so, then Bright Spot 3 is at an earlier stage of cloud evolution than is the Herschel 36, Bright Spot 1 region.

V. M8—A GLOBAL VIEW

We now propose a phenomenological model for the evolutionary history of the NGC 6530–M8 complex. In our scenario, the stars in the cluster were formed about 2×10^6 yr ago at the edge of a massive molecular cloud. Since that time, they have moved away from and/or have severely disrupted the portion of the cloud in which they were born. The remnants of the crater or hole left by these stars in the cloud are visible as the outermost bright-rim structure and low-surface-brightness Hα emission observed toward M8. The excitation for these features is mostly provided by 9 Sgr, an O4f star, toward which a number of the bright rims (including the SEBR) point, and possibly HD 165052, an O7 star, which is located east of the field in Figure 7. This hole, created by the dissipative action of the cluster members, allows the optical observer to see deeper into the molecular cloud, where, possibly, more recent star-forming activity has taken place.

The core of the M8 nebula—which is centered near Herschel 36 and the Hourglass Nebula and is defined by the extent of the most intense radio continuum, CO, infrared, and optical forbidden-line emission—is a region where dissipation and destruction of the remainder of the original cloud are currently taking place. Carbon monoxide, radio continuum, infrared, and strongest forbidden-line emission of [O I], [S II], [N II], [O II], and [O III] all peak near Herschel 36, which suggests that this O7 star is responsible for excitation of the core region. The total radio flux observed toward M8 (Schraml and Mezger 1969) is the same as what would be observed from Orion A if it were at the distance of M8 (2 kpc). Observations of the optical ionization structure in these two nebulae by Dopita (1974) also indicate that the ionization and excitation requirements of the two sources are similar.

Both nebulae emit about the same amount of infrared radiation ($3 \times 10^5 L_\odot$ [Loewenstein *et al.* 1974]). Recent radio observations of Orion A, combined with theoretical predictions for the effective-temperature–luminosity relation for exciting stars, suggest that a star of spectral type O6 is sufficient to account for all the radio flux observed toward Orion A (Caswell and Goss 1974). Thus, the identification of Herschel 36 as the exciting source of M8 would appear consistent as far as energy requirements go. The other likely candidate for the exciting sources is 9 Sgr. Although 9 Sgr is displaced from the center of the H II region, this is not a sufficient reason to dismiss a star as a candidate for an exciting source, as shown in the case of NGC 2024 (Grasdalen 1974). The star 9 Sgr is an O4f star (Conti and Alschuler 1972) and therefore would not be consistent with the observed energy requirements for excitation unless it were at least 5 pc away from the ionized material. At such a distance, it is unlikely that ionization of M8 would be confined to such a small surface of the dark cloud as the region enclosed by SHGS.

The optical observations of § III*c* provide almost compelling evidence for identification of Herschel 36 as the exciting source of the core region. As can be seen in Figures 1 and 7, Herschel 36 is situated within the obscuring matter associated with the SHGS. This matter is probably responsible for most of the 3.5-mag extinction observed toward Herschel 36, implying that both Herschel 36 and the H II region lie behind the SHGS. Only about 0.5 mag of extinction are suffered by 9 Sgr (van Altena and Jones 1972), which strongly implies that Herschel 36 is directly associated with the H II region. If we accept Herschel 36 as the exciting star, then 9 Sgr must be at least 10 pc to the foreground in order not to influence significantly the ionization of the nebula core region.

At present, the nature of the other two CO bright spots is unknown; but if either or both are due to heating by embedded protostars, then they would be considered the most recent star-forming subfragments of the M8 molecular cloud—regions in which the internal sources have not yet had time to disrupt their embryonic material significantly.

Finally, we note that the observed correlation of spatial distribution of radio continuum, Hα, and CO emission indicates that the material in the M8 emission nebula is not uniformly distributed. The lack of Hα or optical emission in the dark lane or Great Rift (Duncan 1920) between SEBR and Herschel 36 (cf. Fig. 7) is not necessarily due to the presence of an absorption lane of foreground material, but is caused by there being less ionized matter in that region, as shown by the radio continuum maps (Ball 1969; Shaver and Goss 1970).

The M8–NGC 6530 complex, which is part of the Sgr OB1 OB association, provides another interesting example of a spatial segregation of association members of different ages (i.e., cluster stars, an H II region, and a molecular cloud) in the same star-forming region. The spatial separation of members of a star-forming complex according to their age is a well-known phenomenon for OB associations (Blaauw 1964). In particular, the Ori OB1 and Cep OB3 associations (cf. Figs. 4 and 6 of Blaauw 1964) are excellent examples. In both cases, the youngest stars are tightly clustered near the boundaries of dark molecular clouds, while the older members are more loosely clustered, gravitationally unbounded, and linearly displaced in galactic longitude from the associated dark clouds. This characteristic of OB associations and related gaseous nebulae suggests that star formation starts at the edge of a large molecular cloud and gradually moves inward, with recently formed stars moving away from and dissipating their placental material as they age. Presumably, this dissipation would take place by ionization and expansion of embryonic material by the more massive members of the association. Unfortunately, the details concerning how stars acquire their expansion velocities and how star formation is initiated and proceeds through a cloud are not yet understood. However, indications are that density-wave theory may provide some answers to the question of the formation of OB associations (Mouschovias *et al.* 1974).

VI. SUMMARY

The most important aspects of our radio and optical observations and their interpretation can be briefly summarized as follows:

1. Three bright spots of CO emission have been uncovered in the central regions of M8.
2. Two of the bright spots are associated in angle with nebular features and far-infrared sources. Bright Spot 1 peaks near the Hourglass Nebula and the star Herschel 36 and is comparable in extent with the core region of ionization in the M8 Nebula. Bright Spot 2 is coincident in angle with a bright-rimmed ionization front southeast of Herschel 36. Bright Spot 3, east of Herschel 36, is apparently not associated with any visible nebular feature.
3. Emission from H_2CO at 140.8 GHz has been detected toward Bright Spot 2 only, indicating that $n_{H_2} \gtrsim 10^4$ cm^{-3} at that location. Weak H_2O emission has also been observed toward this bright spot.
4. Unlike the angular distributions in many other molecular clouds, CO, radio continuum, and optical Hα emission are very similar in angular distribution throughout M8.
5. Radial velocity of CO emission varies smoothly across the molecular cloud but is difficult to interpret in terms of coherent mass motion of the entire cloud.
6. An ionization front in the shape of a large hourglass centered on Herschel 36 is found to be bright in [O I], [O II], [S II], and [N II], but not in [O III] or optical continuum emission.
7. The ionization front coincident with Bright Spot 2 is also found to be bright in [O I], [O II], [S II], and [N II], but not in [O III] or optical continuum emission.
8. Consideration of CO, radio continuum, and, especially, optical data indicates that Herschel 36 is the most likely ionizing source for most of the visible nebula. The H II region appears to be located at the front edge of the molecular cloud, and the ionized gas

is expanding toward the Earth at a velocity of about 7 km s^{-1} with respect to the molecular cloud.

9. The M8 molecular cloud, the M8 H II region, the young cluster NGC 6530, and the Sgr OB1 association appear to be related in a geometrical evolutionary sequence with cloud evolution and, possibly, star formation having proceeded inward from the position of the star cluster to the position of the molecular cloud.

We gratefully acknowledge helpful discussions with R. Loewenstein, D. A. Harper, G. Grasdalen, M. M. Litvak, and A. E. Lilley. We thank J. Ball, B. Baud, D. Dickinson, and H. Penfield for assistance with the observations and M. Hanna for help in preparation of the optical photographs. Radio Astronomy at Harvard is supported in part by NSF grant MPS 74-24063.

REFERENCES

Balick, B., Gammon, R. H., and Hjellming, R. M. 1974, *Pub. A.S.P.*, **86**, 616.
Ball, J. A. 1969, Ph.D. thesis, Harvard University.
Blaauw, A. 1964, *Ann. Rev. Astr. and Ap.*, **2**, 213.
Bohuski, T. J. 1973*a*, *Ap. J.*, **183**, 851.
———. 1973*b*, *Ap. J.*, **184**, 93.
Caswell, J. L., and Goss, W. M. 1974, *Astr. and Ap.*, **32**, 209.
Conti, P. S., and Alschuler, W. R. 1972, *Ap. J.*, **170**, 325.
Davis, J., and Vanden Bout, P. 1973, *Ap. Letters*, **15**, 43.
Dopita, M. A. 1974, *Astr. and Ap.*, **32**, 121.
Duncan, J. C. 1920, *Ap. J.*, **51**, 4.
Foukal, P. 1969, *Astr. and Space Sci.*, **5**, 469.
Gebel, W. L. 1968, *Ap. J.*, **153**, 743.
Giguere, P. T., Snyder, L. E., and Buhl, D. 1973, *Ap. J.* (*Letters*), **182**, L11.
Grasdalen, G. 1974, *Ap. J.*, **193**, 373.
Gull, T. R. 1974, in H II *Regions and the Galactic Center*, Proc. Eighth ESLAB Symposium, A. F. Moorwood, ed., ESRO SP-105, p. 1.
———. 1975, in preparation.
Gull, T. R., and Balick, B. 1974, *Ap. J.*, **192**, 63.
Lada, C. 1975, in preparation.
Lada, C., and Chaisson, E. J. 1975, *Ap. J.*, **195**, 367.
Lada, C., Dickinson, D. F., and Penfield, H. 1974*a*, *Ap. J.*, **189**, 135.
Lada, C. J., Gottlieb, C. A., Litvak, M. M., and Lilley, A. E. 1974*b*, *Ap. J.*, **194**, 609.
Liszt, H. S., Wilson, R. W., Penzias, A. A., Jefferts, K. B., Wannier, P. G., and Solomon, P. M. 1974, *Ap. J.*, **190**, 557.
Loren, R. B., Vanden Bout, P. A., and Davis, J. H. 1973, *Ap. J.* (*Letters*), **185**, L67.
Loewenstein, R. F., Harper, D. A., Thronson, H. A., and Telesco, C. M. 1974, *Bull. A.A.S.*, **6**, 443.
Mouschovias, T. Ch., Shu, F. H., and Woodward, P. R. 1974, *Astr. and Ap.*, **33**, 73.
Reifenstein, E. C., III, Wilson, T. L., Burke, B. F., Mezger, P. G., and Altenhoff, W. 1970, *Astr. and Ap.*, **4**, 357.
Schraml, J., and Mezger, P. G. 1969, *Ap. J.*, **156**, 269.
Shaver, P. A., and Goss, W. M. 1970, *Australian J. Phys. Suppl.*, No. 14, 133.
The, P. S. 1960, *Ap. J.*, **132**, 40.
van Altena, W. F., and Jones, B. F. 1972, *Astr. and Ap.*, **20**, 475.
Walker, M. F. 1957, *Ap. J.*, **125**, 636.
Wilson, T. L., Mezger, P. G., Gardner, F. F., and Milne, D. K. 1970, *Astr. and Ap.*, **6**, 364.
Woolf, N. J. 1961, *Pub. A.S.P.*, **73**, 206.
Woolf, N. J., Stein, W. A., Gillett, F. C., Merrill, K. M., Becklin, E. E., Neugebauer, G., and Pepin, T. J. 1973, *Ap. J.* (*Letters*), **179**, L111.
Zuckerman, B. 1973, *Ap. J.*, **183**, 863.
Zuckerman, B., Buhl, D., Palmer, P., and Snyder, L. E. 1970, *Ap. J.*, **160**, 485.

C. A. GOTTLIEB, E. W. GOTTLIEB, and CHARLES J. LADA: Center for Astrophysics, 60 Garden St., Cambridge, MA 02138

T. R. GULL: Lockheed Electronics Company, 16811-E1 Camino Real, Houston, TX 77058

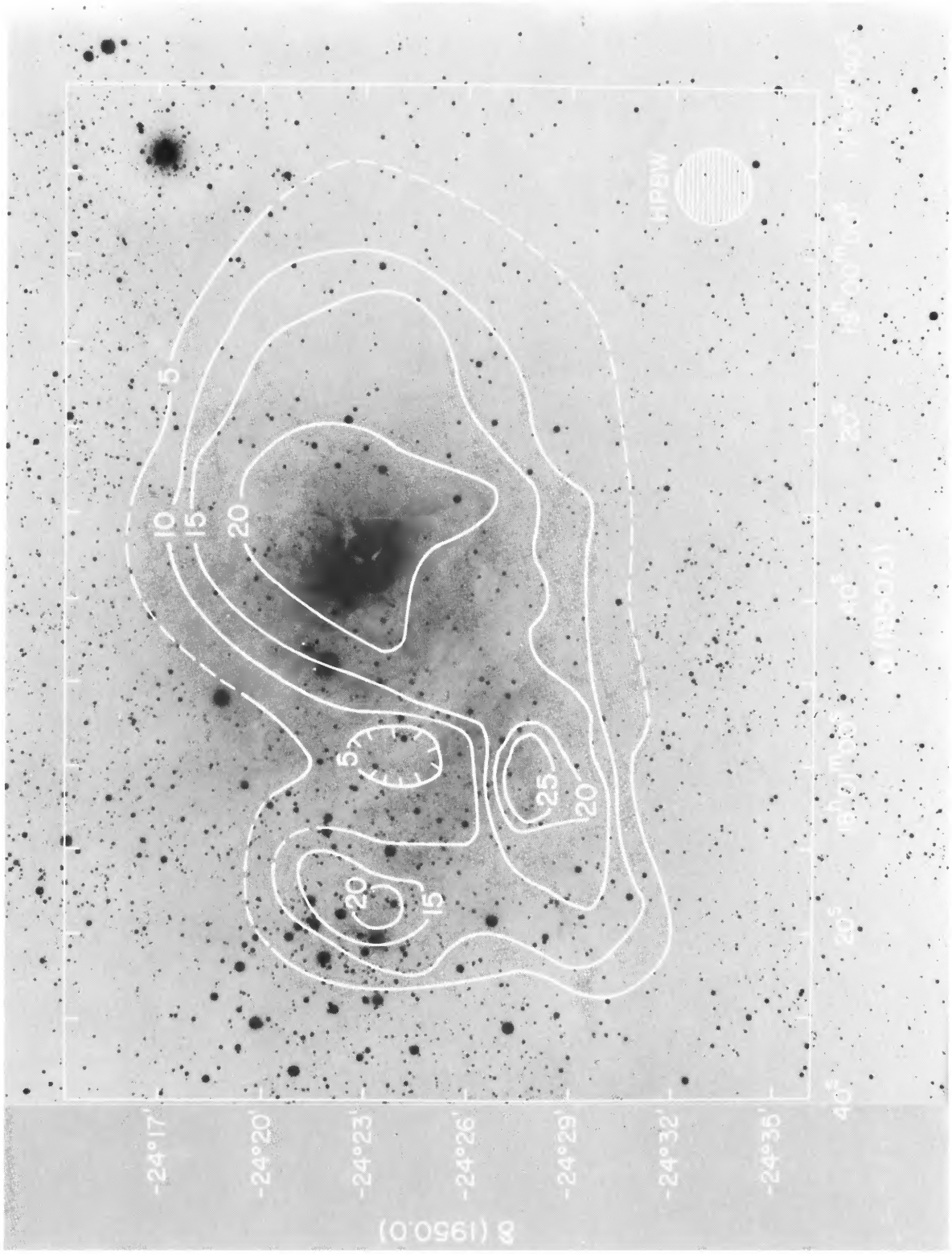

FIG. 1.—Contour map of ^{12}CO apparent Rayleigh-Jeans brightness temperature in kelvins superposed on a prime-focus optical continuum photograph made with the Mayall 4-m telescope through a 90 Å wide interference filter centered at λ6424 in the F/2.6 convergent beam. The exposure time was 1 hour. A 25 K contour approximately 2′ in diameter centered on the star Herschel 36 has been removed to avoid obscuring the detailed optical structure of the inner portions of the visible nebula. The complete map is shown in Fig. 9. The size of the beamwidth of the telescope used to make the ^{12}CO observations is indicated by the disk in the lower right-hand corner.

LADA *et al.* (*see* page 160)

PLATE 6

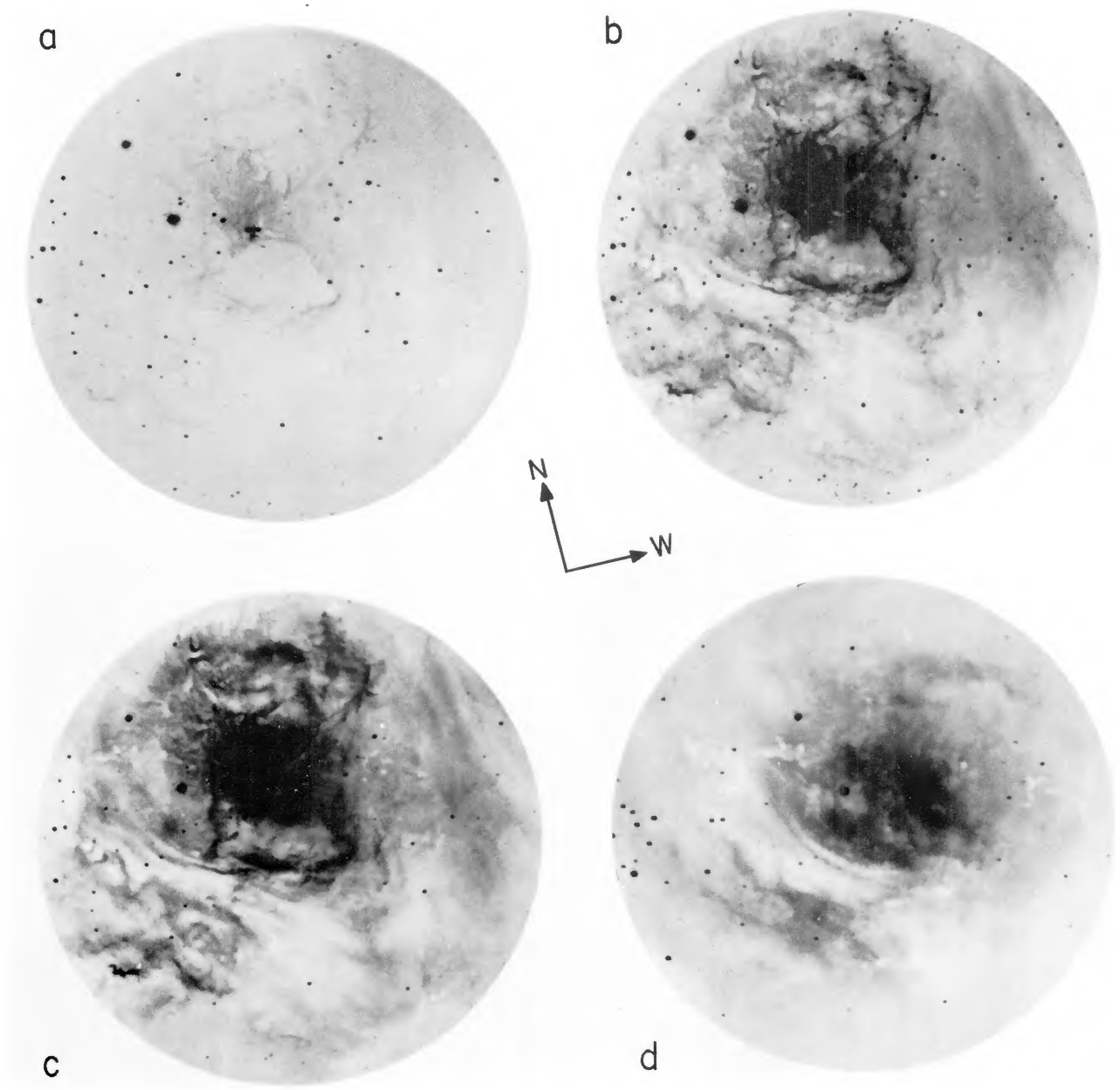

FIG. 8.—Narrow-band interference-filter photographs of the M8 region. These four exposures were taken on the No. 1 92-cm telescope at Kitt Peak at F/7.5 by using a two-stage image intensifier plus IIIaJ emulsions. (*a*) 60-min exposure through a 6 Å wide filter centered at λ6301, recording [O I] (λ6300) emission. (*b*) 20-min exposure through a 25 Å wide filter centered at λ6725, recording [S II] (λ6717 plus λ6731) emission. (*c*) 15-min exposure through a 10 Å wide filter centered at λ6585, recording [N II] (λ6584) emission. (*d*) 10-min exposure through a 20 Å wide filter centered at λ5007, recording [O III] (λ5007) emission.

LADA *et al.* (*see* page 163)

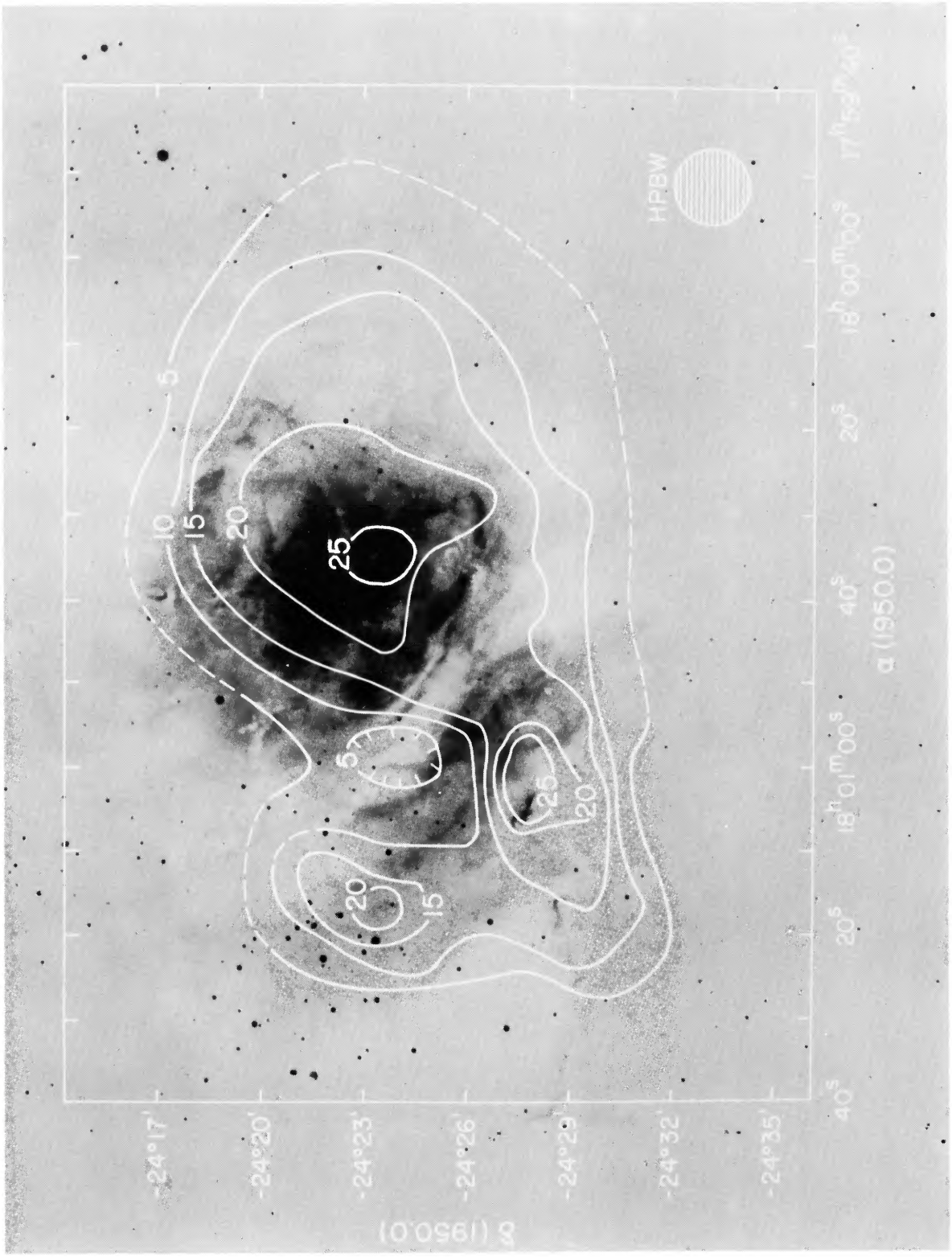

FIG. 9.—Contours of ^{12}CO Rayleigh-Jeans brightness temperature superposed on a photograph of Hα + [N II] emission taken at the prime focus of the 4-m Mayall telescope through a 90 Å wide narrow-band interference filter centered at λ6563 in the F/2.6 convergent beam. The exposure time was 20 min.

LADA *et al.* (*see* page 165)